Hybrid Generalized Modular/Collocation Framework for Distillation Column Synthesis

Petros Proios and Efstratios N. Pistikopoulos
Centre for Process Systems Engineering, Dept. of Chemical Engineering, Imperial College London, London, SW7 2BY U.K.

DOI 10.1002/aic.10711
Published online November 4, 2005 in Wiley InterScience (www.interscience.wiley.com).

Systematic and detailed methods are proposed for the synthesis of simple, heat integrated, and complex distillation column sequences for the separation of non-azeotropic mixtures based on formal superstructure optimization techniques. The Generalized Modular Framework (GMF) developed in previous works for the conceptual synthesis of the aforementioned sequencing problems is enhanced through the incorporation of principles of Collocation techniques for distillation order reduction. The proposed GMF/Collocation methods overcome structural complexities through systematically composed structural models and provide accurate and detailed guidelines for the optimal design and operation of the represented distillation sequences. The synthesis methods are applied for a number of sequencing case studies, generating substantial economic savings by finding systematically, accurately, and in a unified way the most cost efficient distillation column sequence. © 2005 American Institute of Chemical Engineers *AIChE J,* 52: 1038–1056, 2006
Keywords: distillation column sequences, modular framework, GMF, orthogonal collocation

Introduction

The importance of the synthesis of distillation column sequences is inherently related to the extended use of distillation in industry and to the high energy savings that can be achieved through the selection of the most appropriate sequence for a particular separation. In past publications,[1,2] systematic methods were proposed for the synthesis of simple, heat integrated, and complex distillation column sequences at the conceptual level, obtaining the most energy efficient column sequence and generating substantial energy savings. For these purposes, the Generalized Modular Framework[3] was extended with the introduction of novel GMF Structural Models and with the appropriate arrangement of the GMF Physical Model, for the structural generation and physical representation of distillation sequences. The GMF Structural Models incorporated logical modeling principles, while the GMF Physical Model was based on aggregation techniques. The synthesis methods generating systematically and automatically all the structural alternatives and avoiding common structural and physical simplifying assumptions, obtained the most energy efficient column arrangements validly capturing the underlying physical phenomena while generating significantly compact optimization problems to solve. The proposed methods treated the synthesis problems at the conceptual level, focusing on higher-level design targets (optimal energy consumption and column sequence selection), leaving lower-level design targets, such as the columns' dimensioning (trays, diameters), at a later stage. This did not affect the usefulness of the GMF methods proposed for the synthesis of energy efficient distillation column sequences since it is well established that the operating cost (energy consumption) constitutes the main synthesis driving force in the distillation sequencing problem. This is due to the fact that the capital cost contribution to the Total Annualized Cost (TAC) of distillation systems is significantly smaller than that of the operating cost (20% as opposed to 80%, according to Douglas[4]). The GMF obtained the most energy efficient column sequences due to its valid operating cost estimates, as validated over comparisons to rigorous distillation models.

However, it remains a challenge to enhance the GMF Phys-

Correspondence concerning this article should be addressed to E. N. Pistikopoulos at e.pistikopoulos@imperial.ac.uk.

ical Model so that it can incorporate column dimensionality and intra-module information without sacrificing the GMF's main advantages of size compactness and representation efficiency achieved due to avoiding the use of shortcut models or simplifying assumptions. The use of Kremser Group Methods cannot be employed for this purpose, since these are based on simplifying assumptions of sharp splits, equimolar flowrates, isothermal operation, and linear phase equilibrium relations, assumptions that can be potentially limiting.[5] Moreover, the shortcut models do not provide intra-column information (for instance, on temperature or composition profiles). This must be obtained through interpolation between the section ends providing only rough estimates, thus limiting the models' detail and accuracy levels. At the same time, employing rigorous tray-by-tray MINLP models can provide accurate physical representations but at a substantial increase of the continuous and combinatorial size of the generated problem, leading to the loss of the GMF's advantage of compactness.

An approach that can guarantee the safeguarding of the aforementioned GMF physical representation advantages and can still achieve the GMF Physical Model enhancement is the use of principles of Order Reduction Methods for distillation, namely, those of Orthogonal Collocation (OC) and Orthogonal Collocation on Finite Elements (OCFE). Collocation methods were first proposed for distillation order reduction by Cho and Joseph,[6] who proposed a method for steady state and dynamic distillation models based on the idea of approximating a staged distillation column as a distributed system in which the composition and flowrates were approximated by Lagrange polynomials, over collocation points defined as the zeros of orthogonal Jacobi polynomials. The method was developed for single gas absorption columns and was extended to simple distillation columns in Cho and Joseph[7] and to distillation columns with side streams in Cho and Joseph.[8] Stewart et al.[9] proposed an orthogonal collocation technique for steady state and dynamic simulations of distillation systems, based on the approximation of the system states (molar fractions and enthalpies) in each column section, also by Lagrange polynomials that were fitted to the process model at collocation points chosen as the zeros of the Hahn family of polynomials obeying orthogonality conditions. The accuracy of using Hahn polynomials was demonstrated through a number of case studies. Furthermore, the proposed method proved more advantageous and consistent than other order reduction methods, such as the Laplace-Domain lumping,[10] the Time-Domain lumping,[11] and the Compartmental lumping.[12] Swartz and Stewart[13] extended the above method to the distillation design problem, where the continuous number of stages (as incorporated in the collocation scheme) was determined directly by the optimization. The optimization results were found to be in very good agreement with conventional distillation design methods. In Swartz and Stewart,[14] a Finite Element Collocation scheme was used in order to predict the phase boundaries of multiphase distillation systems. Seferlis and Hrymak,[15] based on the above methods, proposed systematic and detailed OC and OCFE design methods for single distillation columns. The method proved to be in excellent agreement with the rigorous models. Moreover, the authors provided an approximation error analysis, where different discretization schemes (combinations of different numbers of Finite Elements and Collocation Points) were compared for the minimization of the approximation error. The optimal Element length issue was further addressed in Seferlis and Hrymak,[16] based on the approximation error equidistribution. A collocation method for distillation was also proposed by Huss and Westerberg,[17] who broke each column section into two Elements of two collocation "trays." Lagrange approximation polynomials were used and the collocation points were the roots of appropriately weighted orthogonal Jacobi polynomials. In order to provide better approximations for large columns where difficult separations took place, the authors proposed appropriate variable transformations.

This collocation model was applied in Huss and Westerberg,[18] followed by a systematic solution procedure, for minimum reflux and Total Annualized Cost calculations and optimizations for single distillation columns. More recently, Zhang and Linninger[19] proposed a new minimum bubble point distance (MIDI) algorithm for addressing the feasibility problem of distillation separations, employing collocation techniques. Based on the conversion of the tray-by-tray difference equations into ordinary differential equations (ODE) over the column height,[20] the authors proposed a mapping of the column height into a dimensionless bubble point temperature, thus expressing the ODEs for the component compositions over the bubble point temperature instead of the column height. The ODEs were then converted into algebraic equations using orthogonal collocation on finite elements and Lagrange and Legendre base polynomials.

As reported in the literature, the OC and OCFE methods for distillation order reduction can provide accurate intra-section detail and tray number estimates in a compact and modular way. This provided the key for the GMF Physical Model enhancement target. In this article the GMF Physical Model will be coupled to principles of the OC and OCFE methods in order to enhance the GMF physical representations with components of a simulation tool, obtaining detailed intra-module information and column design guidelines, while preserving the GMF's combinatorial and continuous compactness. The proposed GMF/Collocation Physical Models coupled to the appropriate GMF Structural Models will provide accurate and detailed GMF-based methods for the synthesis of simple, heat integrated, and complex distillation column sequences, obtaining the most cost efficient column sequence and generating substantial economic savings. The main principles and validity of the proposed synthesis methods will be demonstrated over the examination of illustrating case studies.

Problem Statement

The target of this work is the enhancement of the GMF Synthesis Models for the synthesis of simple, heat integrated, and complex distillation column sequences by incorporating in the GMF Physical Model principles from the Orthogonal Collocation (OC) and Orthogonal Collocation on Finite Elements (OCFE) methods for order reduction of distillation models. For this purpose, the GMF Synthesis Models proposed in Proios and Pistikopoulos[1] and Proios et al.[2] will be coupled to the OC and OCFE methods proposed by Seferlis and Hrymak,[15] which have been reported to be able to efficiently address the single column distillation design problem based on highly accurate physical representations, comparable to those obtained by rigorous models. Two formal synthesis methods, namely, the GMF/OC and the GMF/OCFE, will be proposed, obtaining the

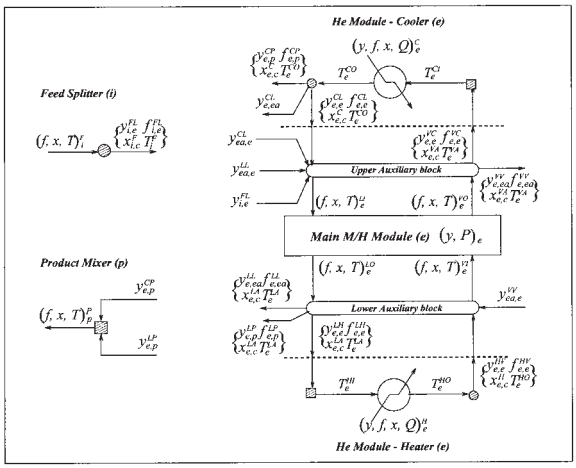

Figure 1. GMF building blocks for distillation representation and sequencing.

optimal column sequence capturing *simultaneously* interactions between optimal column design and operation. The proposed synthesis methods will allow for accurate representations of the underlying physical phenomena and for detailed sequencing designs to be obtained with information about the columns' dimensions (trays, diameters, and so on) while maintaining the GMF's combinatorial and continuous compactness. This will provide a framework for evaluating in a unified way the economic benefits obtained by the use of simple, heat integrated, and thermally coupled distillation columns. Moreover, the proposed synthesis methods will be used to *explicitly* represent and capture the economic advantages of particular designs, such as the Dividing Wall Column. From a computational point of view, the OC and OCFE principles will be incorporated appropriately in the GMF, allowing the use of each GMF-based Physical Model (GMF, GMF/OC or GMF/OCFE) according to the synthesis problem solved and the representational detail desired.

GMF/OC Physical Model

The GMF Physical Model is used for the representation of the physical phenomena taking place within the structural alternatives generated by the GMF Structural Model. These alternatives, which are essentially combinations of appropriately interconnected GMF Building Blocks, are physically evaluated with respect to their feasibility (ability to meet the problem specifications) and their optimality with respect to the design targets. The GMF Physical Model is constructed by the respective physical models of the GMF Building Blocks, which are categorized into two types, namely, the Mass/Heat (*M/H*) and the Pure Heat (*He*) modules. Other GMF structural components, such as feed splitters and product mixers, are also accompanied by appropriate physical models. The GMF Building Blocks and other structural components are shown in Figure 1.

It must be pointed out that each *M/H* module consists of an Upper and Lower Auxiliary Block and of a Main *M/H* block. For the distillation representation/sequencing problems, the Main *M/H* block represents column sections (clusters of trays) and the *He* modules (coolers and heaters) represent column condensers and reboilers. A presentation and discussion of the physical models of these GMF Building Blocks and structural constraints can be found in detail in Proios and Pistikopoulos.[1] The *M/H* modules, due to their aggregation, utilize information on the modules' boundaries, leading to the generation of considerably compact problems to solve. In general, their physical models are based on fundamental (and thus general) mass and heat exchange principles, incorporating mass and energy balances along with Phase Defining and Driving Force Constraints, appropriately defined in order to arrange the mass and heat transfer. Through comparisons to rigorous distillation models, these physical models proved capable of validly capturing the general mass and heat transfer trends in the various distillation column sections. In this work, novel GMF Physical Models are proposed incorporating principles of orthogonal collocation techniques for distillation order reduction.

A full order model for a distillation column considers information (variables and equations) at points that correspond to each column tray. This model corresponds to a rigorous tray-by-tray model (for instance, that of Viswanathan and Grossmann[21]), which essentially "discretizes" a column into trays. The main rationale behind an Orthogonal Collocation (OC) model for distillation, like the one proposed by Seferlis and Hrymak,[15] is that information is considered at fewer points than the full order model, thus generating a problem with less variables and constraints. This is achieved by approximating certain variables in each column section with Lagrange polynomials. The latter are defined at certain (collocation) points, whose number depends on the order of the polynomials. The number of interior collocation points should be less than or equal to the number of trays in the section.

For the incorporation of the OC method of Seferlis and Hrymak[15] in the GMF, each Main *M/H* block of M_e trays corresponds to a single Element of "*length*" $M_e + 1$ (counting trays from top to bottom, $M_e + 1$ is the tray that provides the vapor inlet stream to the examined section, while index *e* refers to the discretized *M/H* module). According to the order of the approximating Lagrange polynomials, the Main *M/H* block is discretized into $nc_e + 2$ collocation points ($j=0,1,\ldots,nc_e,nc_e+1$), as shown in Figure 2. The location, $s_{e,j}$, of each collocation point corresponds to a tray number. The collocation points *0* and nc_e+1 are called exterior collocation points, and their locations are at the Element's origin ($s_{e,(j=0)} = s_{e,0} = 0$) and at its end ($s_{e,(j=nc_e+1)} = s_{e,nc_e+1} = M_e+1$). The locations of the interior (remaining) collocation points are defined by the roots of appropriate polynomials obeying orthogonality conditions. For the mapping of collocation points, Stewart et al.[9] compared alternative families of polynomials for their accuracy for the representation of distillation column behavior. From that study it was found that appropriately weighted Hahn polynomials were the most adequate for trayed distillation column approximation and that, if the order of the approximating polynomials is equal to the number of trays in a column section, then the full order model is obtained. The authors also provided the resulting roots, which are explicit functions of the "*length*" (number of trays), for up to 4 interior collocation points.

For illustration, the case of 1 ($nc_e = 1$) interior collocation point is shown below:

$$s_{e,(j=0)} = s_{e,0} = 0 \tag{1}$$

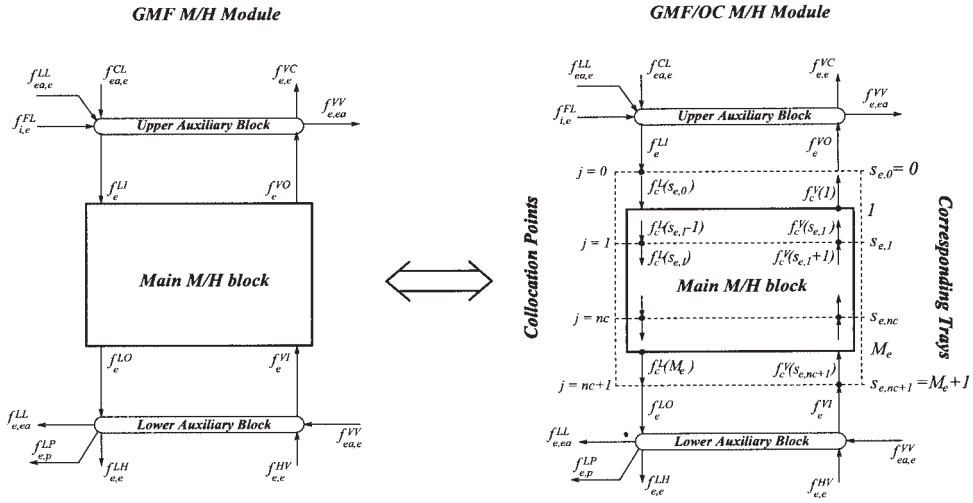

Figure 2. GMF and GMF/OC *M/H* module for distillation.

$$s_{e,(j=nc)} = s_{e,1} = \frac{M_e + 1}{2} \tag{2}$$

$$s_{e,(j=nc_e+1)} = s_{e,2} = M_e + 1 \tag{3}$$

Once the order of the approximating Lagrange polynomials is assigned (number of collocation points), the latter are used for the approximation of the liquid and vapor component molar flowrates and enthalpies. For illustration purposes, the Lagrange polynomial approximation expressions for the liquid and vapor component flowrates for a location s_e in the Main *M/H* block are given in Eqs. 4 and 5. These are expressed in terms of the discretized liquid and vapor component flowrates $fc_c^L(s_{e,j})$ and $fc_c^V(s_{e,j})$ over the collocation points j.

$$fc_c^L(s_e) = \sum_{j=0}^{nc_e} W_j^L(s_e)\, fc_c^L(s_{e,j}), \quad c \in C \tag{4}$$

$$fc_c^V(s_e) = \sum_{j=1}^{nc_e+1} W_j^V(s_e)\, fc_c^V(s_{e,j}), \quad c \in C \tag{5}$$

The polynomial approximations for the enthalpies are written in an similar form. It must be noted that in the above expressions the liquid flowrates are defined over nc_e+1 collocation points ($fc_c^L(s_{e,0}), \ldots, fc_c^L(s_{e,nc_e})$) whereas the vapor flowrates are defined over a different set of nc_e+1 collocation points ($fc_c^V(s_{e,1}), \ldots, fc_c^V(s_{e,nc_e+1})$). The dependence of the approximating polynomials on the location of the examined point, s_e, and on the total "*length*" (number of trays) of the Main *M/H* block is included in the Lagrange polynomials $W_j^L(s_e)$ and $W_j^L(s_e)$:

$$W_j^L(s_e) = \prod_{z=0,j}^{nc_e} \frac{s_e - s_{e,z}}{s_{e,j} - s_{e,z}}, \quad j = 0, \ldots, nc_e \tag{6}$$

$$W_j^V(s_e) = \prod_{z=1,j}^{nc_e+1} \frac{s_e - s_{e,z}}{s_{e,j} - s_{e,z}}, \quad j = 1, \ldots, nc_e + 1 \tag{7}$$

In the above, $s_{e,z}$ and $s_{e,j}$ are expressed as functions of the number of trays (M_e) using relations like Eqs. 1 to 3, according to the number of collocation points used. Substituting the approximating polynomials into the *MESH* distillation column equations yields a corresponding set of residual functions continuous in s_e. The collocation equations of the GMF/OC model are then derived by setting these residual functions equal to zero at the *interior* collocation points ($s_{e,1}, \ldots, s_{e,nc}$). Therefore, the number of GMF/OC model variables and equations depends exclusively on the number of sections in the column and on the number of collocation points per section. For illustration, the component mass balances are given below:

$$fc_c^V(s_{e,j}+1) + fc_c^L(s_{e,j}-1) - fc_c^V(s_{e,j}) - fc_c^L(s_{e,j}) = 0, \quad c \in C, \quad j = 1, \ldots, nc_e \tag{8}$$

In these balances the location, $s_{e,j}$, of each collocation point j corresponds to a tray number (which could be an integer or not). Therefore, the locations $s_{e,j} + 1$ and $s_{e,j} - 1$ correspond to the following and previous trays of tray $s_{e,j}$, providing the inlet vapor and liquid streams to this "tray" $s_{e,j}$. However, since these locations do not correspond to collocation points, their respective component flowrates have to be interpolated using the polynomial approximations of Eqs. 4 and 5. Thus, the component mass balances become:

$$\sum_{j'=1}^{nc_e+1} W_{j'}^V(s_{e,j}+1)\, fc_c^V(s_{e,j'}) + \sum_{j'=0}^{nc_e} W_{j'}^L(s_{e,j}-1)\, fc_c^L(s_{e,j'}) - fc_c^V(s_{e,j}) - fc_c^L(s_{e,j}) = 0, \quad c \in C, \quad j = 1, \ldots, nc_e \tag{9}$$

Index j' refers also to collocation points and is used as a separate interior counter in the summations. Using Eqs. 6 and

7, the W functions over the locations $s_{e,j}+1$ and $s_{e,j}-1$, are given below:

$$W_{j'}^{L}(s_{e,j}-1)=\prod_{z=0,j'}^{nc_e}\frac{(s_{e,j}-1)-s_{e,z}}{s_{e,j'}-s_{e,z}},\quad j=1,\ldots,nc_e \tag{10}$$

$$W_{j'}^{V}(s_{e,j}+1)=\prod_{z=1,j'}^{nc_e+1}\frac{(s_{e,j}+1)-s_{e,z}}{s_{e,j'}-s_{e,z}},\quad j=1,\ldots,nc_e \tag{11}$$

The outlet vapor and liquid streams leaving each Main *M/H* block should be written in their polynomial form. This is because the origin of those streams does not correspond to collocation points (first, topmost, tray for the vapor stream $fc_c^V(1)$, and last (M_e), lowermost, tray for the liquid stream, $fc_c^L(M_e)$). These streams participate in their polynomial form in the balances of the Upper and Lower Auxiliary Blocks on the two sides of the Main *M/H* block. The inlet vapor and liquid streams entering each Main *M/H* block correspond to the block's exterior collocation points, not requiring a polynomial extrapolation, and are made equal to the corresponding Auxiliary Block's outlet streams.

The GMF/OC Physical Model is based on the GMF model of Proios and Pistikopoulos.[1] From the latter, the models of the Feed Splitter, Upper and Lower Auxiliary blocks, Cooler and Heater blocks, and Product Mixer remain exactly the same. The only part of the GMF Physical Model where the GMF/OC constraints are introduced is the Main *M/H* block. Also, additional equality constraints are used in order to link the GMF/OC Main *M/H* block model to the GMF Auxiliary block models using the appropriate polynomial approximations specified above. The GMF/OC constraints are characterized as *substituting* and *supplementary*, depending on whether they substitute or are added to the constraints of the GMF model. A discussion of this formulation follows later in the article.

GMF/OC main M/H *block physical model (*substituting*)*

The presented model should effectively *substitute* the Main *M/H* block Physical Model in Proios and Pistikopoulos.[1] It consists of: the discretized *MESH* equations (enforced at the interior collocation points), the mixed integer physical-structural constraints, and the equations that relate the collocation point locations, $s_{e,j}$, and the Lagrange polynomial weighting functions, $W_j^L(s_e)$ and $W_j^V(s_e)$, to the number of trays, M_e, per *M/H* block e.

–Collocation Point Locations and Weighting Functions

$$s_{e,0}-1=0,\quad e\in E^E \tag{12}$$

$$s_{e,j}-s_j(M_e)=0,\quad e\in E^E,\ j=1,\ldots,nc_e \tag{13}$$

$$s_{e,nc_e+1}-(M_e+1)=0,\quad e\in E^E \tag{14}$$

$$W_{j'}^{V}(s_e)-\prod_{z=1,j'}^{nc_e+1}\frac{s_e-s_{e,z}}{s_{e,j'}-s_{e,z}}=0,\quad e\in E^E,\ j'=1,\ldots,nc_e+1 \tag{15}$$

$$W_{j'}^{L}(s_e)-\prod_{z=0,j'}^{nc_e}\frac{s_e-s_{e,z}}{s_{e,j'}-s_{e,z}}=0,\quad e\in E^E,\ j'=0,\ldots,nc_e \tag{16}$$

–Component Mass and Energy Balances

$$\sum_{j'=1}^{nc_e+1}W_{j'}^{V}(s_{e,j}+1)\,fc_c^V(s_{e,j'})+\sum_{j'=0}^{nc_e}W_{j'}^{L}(s_{e,j}-1)\,fc_c^L(s_{e,j'})-fc_c^V(s_{e,j})-fc_c^L(s_{e,j})=0,\quad e\in E^E,\ c\in C,\ j=1,\ldots,nc_e \tag{17}$$

$$\sum_{j'=1}^{nc_e+1}W_{j'}^{V}(s_{e,j}+1)\,f^V(s_{e,j'})h^V(s_{e,j'})+\sum_{j'=0}^{nc_e}W_{j'}^{L}(s_{e,j}-1)\,f^L(s_{e,j'})h^L(s_{e,j'})-f^V(s_{e,j})h^V(s_{e,j})-f^L(s_{e,j})h^L(s_{e,j})=0,\quad e\in E^E,\ j=1,\ldots,nc_e \tag{18}$$

–Phase Equilibrium

$$\left[\frac{fc_c^V(s_{e,j})}{f^V(s_{e,j})}\right]-K_c(s_{e,j})\left[\frac{fc_c^L(s_{e,j})}{f^L(s_{e,j})}\right]=0,\quad e\in E^E,\ c\in C,\ j=1,\ldots,nc_e \tag{19}$$

–Molar Fraction Summations

$$\sum_{c\in C}\frac{fc_c^V(s_{e,j})}{f^V(s_{e,j})}-1=0,\quad e\in E^E,\ j=1,\ldots,nc_e \tag{20}$$

$$\sum_{c\in C}\frac{fc_c^L(s_{e,j})}{f^L(s_{e,j})}-1=0,\quad e\in E^E,\ j=1,\ldots,nc_e \tag{21}$$

–Mixed Integer Physical-Structural Constraints

$$f_e^{LO}-y_e\mathcal{F}^{\max}\le 0,\quad e\in E \tag{22}$$

$$f_e^{LI}-y_e\mathcal{F}^{\max}\le 0,\quad e\in E \tag{23}$$

$$f_e^{VO}-y_e\mathcal{F}^{\max}\le 0,\quad e\in E \tag{24}$$

$$f_e^{VI}-y_e\mathcal{F}^{\max}\le 0,\quad e\in E \tag{25}$$

$$f^L(s_{e,j})-y_e\mathcal{F}^{\max}\le 0,\quad e\in E,j=0,\ldots,nc_e \tag{26}$$

$$f^V(s_{e,j})-y_e\mathcal{F}^{\max}\le 0,\quad e\in E,j=1,\ldots,nc_e+1 \tag{27}$$

Conditions linking upper auxiliary block (supplementary)

The following *supplementary* equations link the physical model of the Main *M/H* block (GMF/OC) to that of the Upper Auxiliary block (GMF). They represent a relation between the GMF/OC and GMF inputs and outputs in the top part of the *M/H* Module.

$$f_e^{VO} - \sum_{c\in C}\left(\sum_{j=1}^{nc_e+1} W_j^V(1)\, fc_c^V(s_{e,j})\right) = 0, \quad e \in E^E \tag{28}$$

$$f_e^{LI} - f^L(s_{e,0}) = 0, \quad e \in E^E \tag{29}$$

$$f_e^{VO} x_{e,c}^{VO} - \sum_{j=1}^{nc_e+1} W_j^V(1)\, fc_c^V(s_{e,j}) = 0, \quad e \in E^E,\ c \in C \tag{30}$$

$$f_e^{LI} x_{e,c}^{LI} - fc_c^L(s_{e,0}) = 0, \quad e \in E^E,\ c \in C \tag{31}$$

$$f_e^{VO} h_e^{VO} - \sum_{j=1}^{nc_e+1} W_j^V(1)\, f^V(s_{e,j}) h^V(s_{e,j}) = 0, \quad e \in E^E \tag{32}$$

$$f_e^{LI} h_e^{LI} - f^L(s_{e,0}) h^L(s_{e,0}) = 0, \quad e \in E^E \tag{33}$$

*Conditions linking lower auxiliary block (***supplementary***)*

Similar to the Upper Auxiliary block, *supplementary* equations should be *added* to the GMF Physical Model, relating the GMF Lower Auxiliary block physical model to that of the GMF/OC Main *M/H* block (inputs and outputs in the lower part of the *M/H* module).

$$f_e^{LO} - \sum_{c\in C}\left(\sum_{j=0}^{nc_e} W_j^L(M_e)\, fc_c^L(s_{e,j})\right) = 0, \quad e \in E^E \tag{34}$$

$$f_e^{VI} - f^V(s_{e,nc_e+1}) = 0, \quad e \in E^E \tag{35}$$

$$f_e^{LO} x_{e,c}^{LO} - \sum_{j=0}^{nc_e} W_j^L(M_e)\, fc_c^L(s_{e,j}) = 0, \quad e \in E^E,\ c \in C \tag{36}$$

$$f_e^{VI} x_{e,c}^{VI} - fc_c^V(s_{e,nc_e+1}) = 0, \quad e \in E^E,\ c \in C \tag{37}$$

$$f_e^{LO} h_e^{LO} - \sum_{j=0}^{nc_e} W_j^L(M_e)\, f^L(s_{e,j}) h^L(s_{e,j}) = 0, \quad e \in E^E \tag{38}$$

$$f_e^{VI} h_e^{VI} - f^V(s_{e,nc_e+1}) h^V(s_{e,nc_e+1}) = 0, \quad e \in E^E \tag{39}$$

*Thermodynamic functions (***supplementary***)*

These *supplementary* equations relate the discretized enthalpies and equilibrium constants to the discretized temperatures and vapor and liquid molar fractions. They should be *added* to the GMF Physical Model thermodynamic functions. Any thermodynamic model can be readily used for their calculation.

$$H^V(s_{e,j}) - H^V\left(\frac{fc^V}{f^V}, T\right)_{(s_{e,j})} = 0, \quad e \in E^E,\ j = 1, \ldots, nc_e + 1 \tag{40}$$

$$H^L(s_{e,j}) - H^L\left(\frac{fc^L}{f^L}, T\right)_{(s_{e,j})} = 0, \quad e \in E^E,\ j = 0, \ldots, nc_e \tag{41}$$

$$K_c(s_{e,j}) - K_c\left(\frac{fc_c^L}{f^L}, \frac{fc_c^V}{f^V}, T, P\right)_{(s_{e,j})} = 0, \quad e \in E^E,\ c \in C,\ j = 1, \ldots, nc_e \tag{42}$$

GMF/OCFE Physical Model

In the OC method for distillation, each column section corresponded to a single Element, discretized into a number of collocation points. It is possible, though, to have profiles within the same column section that are fairly flat over a number of trays, thus requiring a small number of collocation points to capture the physical behavior, and other parts that exhibit very steep profiles, thus requiring either a greater number of collocation points or collocation points more closely positioned. In order to achieve this, either a large number of collocation points can be used, or the column section can be broken into more than one Finite Element. The first case can be viewed as a rather crude approach, which also increases the size of the problem without necessarily capturing the detail in the crucial parts of each section. On the contrary, the second approach is the one recommended for this purpose. This method is called Orthogonal Collocation On Finite Elements (OCFE). The flexibility of this method is that the column section can be broken into Finite Elements with fewer collocation points for flat profile regions and into Finite Elements with more collocation points or with smaller lengths for steep profile regions.

In Seferlis and Hrymak,[15] an OCFE method was also proposed, which is incorporated in the GMF Physical Model as an extension of the GMF/OC method. In general, each Main *M/H* block is "broken" into l Finite Elements, each of a length $M_{e,l}$ (number of trays) and each discretized into a specified number of collocation points, as shown in Figure 3. Each Finite Element is governed by the same conditions as the single Element of the GMF/OC method and, therefore, the GMF/OCFE model is based on that of the GMF/OC and composed in the same way, consisting of *substituting* and *supplementary* equations. The only additional (*supplementary*) condition is that of zero-order continuity between adjacent Finite Elements for the component liquid and vapor flow rates and enthalpies. Also, the GMF/OCFE variables are written with an additional index (l) denoting the Finite Element over which they are defined. For this purpose a new set L_e is introduced:

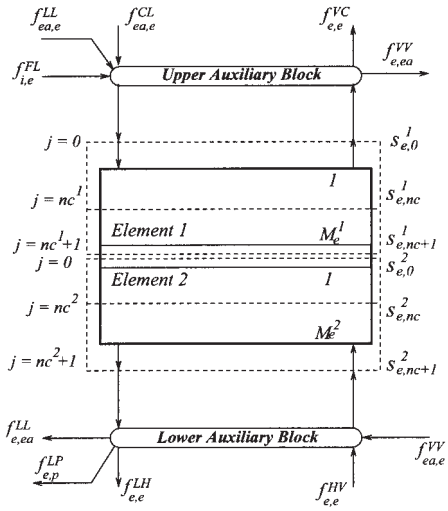

Figure 3. GMF/OCFE Main *M/H* block discretization.

$$L_e = \{l | number\ of\ Finite\ Elements\ per\ module\ e\}$$

GMF/OCFE main M/H *block physical model* (substituting)

–Collocation Point Locations and Weighting Functions per Element

$$s_{e,l,0} - 1 = 0, \quad e \in E^E,\ l \in L_e \tag{43}$$

$$s_{e,l,j} - s_j(M_{e,l}) = 0, \quad e \in E^E,\ l \in L_e,\ j = 1, \ldots, nc_{e,l} \tag{44}$$

$$s_{e,l,nc_{e,l}+1} - (M_{e,l} + 1) = 0, \quad e \in E^E,\ l \in L_e \tag{45}$$

$$W_{j'}^V(s_{e,l}) - \prod_{z=1,j'}^{nc_{e,l}+1} \frac{s_{e,l} - s_{e,l,z}}{s_{e,l,j'} - s_{e,l,z}} = 0, \quad e \in E^E,\ l \in L_e,\ j' = 1, \ldots, nc_{e,l} + 1 \tag{46}$$

$$W_{j'}^L(s_{e,l}) - \prod_{z=0,j'}^{nc_{e,l}} \frac{s_{e,l} - s_{e,l,z}}{s_{e,l,j'} - s_{e,l,z}} = 0, \quad e \in E^E,\ l \in L_e,\ j' = 0, \ldots, nc_{e,l} \tag{47}$$

–Component Mass and Energy Balances

$$\sum_{j'=1}^{nc_{e,l}+1} W_{j'}^V(s_{e,l,j} + 1)\, fc_c^V(s_{e,l,j'}) + \sum_{j'=0}^{nc_{e,l}} W_{j'}^L(s_{e,l,j} - 1)\, fc_c^L(s_{e,l,j'}) - fc_c^V(s_{e,l,j}) - fc_c^L(s_{e,l,j}) = 0, \quad e \in E^E,\ l \in L_e,\ j = 1, \ldots, nc_{e,l},\ c \in C \tag{48}$$

$$\sum_{j'=1}^{nc_{e,l}+1} W_{j'}^V(s_{e,l,j} + 1)\, f^V(s_{e,l,j'}) h^V(s_{e,l,j'}) + \sum_{j'=0}^{nc_{e,l}} W_{j'}^L(s_{e,l,j} - 1) f^L(s_{e,l,j'}) h^L(s_{e,l,j'}) - f^V(s_{e,l,j}) h^V(s_{e,l,j}) - f^L(s_{e,l,j}) h^L(s_{e,l,j}) = 0, \quad e \in E^E,\ l \in L_e,\ j = 1, \ldots, nc_{e,l} \tag{49}$$

–Phase Equilibrium

$$\left[\frac{fc_c^V(s_{e,l,j})}{f^V(s_{e,l,j})}\right] - K_c(s_{e,l,j})\left[\frac{fc_c^L(s_{e,l,j})}{f^L(s_{e,l,j})}\right] = 0, \quad e \in E^E,\ l \in L_e,\ j = 1, \ldots, nc_{e,l},\ c \in C \tag{50}$$

–Molar Fraction Summations

$$\sum_{c \in C} \frac{fc_c^V(s_{e,l,j})}{f^V(s_{e,l,j})} - 1 = 0, \quad e \in E^E,\ l \in L_e,\ j = 1, \ldots, nc_{e,l} \tag{51}$$

$$\sum_{c \in C} \frac{fc_c^L(s_{e,l,j})}{f^L(s_{e,l,j})} - 1 = 0, \quad e \in E^E,\ l \in L_e,\ j = 1, \ldots, nc_{e,l} \tag{52}$$

–Mixed Integer Physical-Structural Constraints

$$f_e^{LO} - y_e \mathcal{F}^{\max} \le 0, \quad e \in E \tag{53}$$

$$f_e^{LI} - y_e \mathcal{F}^{\max} \le 0, \quad e \in E \tag{54}$$

$$f_e^{VO} - y_e \mathcal{F}^{\max} \le 0, \quad e \in E \tag{55}$$

$$f_e^{VI} - y_e \mathcal{F}^{\max} \le 0, \quad e \in E \tag{56}$$

$$f^L(s_{e,l,j}) - y_e \mathcal{F}^{\max} \le 0, \quad e \in E,\ l \in L_e,\ j = 0, \ldots, nc_{e,l} \tag{57}$$

$$f^V(s_{e,l,j}) - y_e \mathcal{F}^{\max} \le 0, \quad e \in E,\ l \in L_e,\ j = 1, \ldots, nc_{e,l} + 1 \tag{58}$$

Conditions linking adjacent finite elements (supplementary)

$$\sum_{c \in C} \left(\sum_{j=0}^{nc_{e,l-1}} W_j^L(M_{e,l-1})\, fc_c^L(s_{e,l-1,j}) \right) - f^L(s_{e,l,0}) = 0, \quad e \in E^E,\ l = 2, \ldots, |L_e| \tag{59}$$

$$f^V(s_{e,l-1,nc^{e,l-1}+1}) - \sum_{c \in C} \left(\sum_{j=1}^{nc_{e,l}+1} W_j^V(1)\, fc_c^V(s_{e,l,j}) \right) = 0, \quad e \in E^E,\ l = 2, \ldots, |L_e| \tag{60}$$

$$\sum_{j=0}^{nc_{e,l-1}} W_j^L(M_{e,l-1})\, fc_c^L(s_{e,l-1,j}) - fc_c^L(s_{e,l,0}) = 0, \quad e \in E^E,\ l = 2, \ldots, |L_e|,\ c \in C \tag{61}$$

$$fc_c^V(s_{e,l-1,nc^{e,l-1}+1}) - \sum_{j=1}^{nc_{e,l}+1} W_j^V(1)\, fc_c^V(s_{e,l,j}) = 0, \quad e \in E^E, \quad l = 2, \ldots, |L_e|, \; c \in C \tag{62}$$

$$\sum_{j=0}^{nc_{e,l-1}} W_j^L(M_{e,l-1})\, f^L(s_{e,l-1,j})\, H^L(s_{e,l-1,j}) - f^L(s_{e,l,0})\, H^L(s_{e,l,0}) = 0, \quad e \in E^E, \; l = 2, \ldots, |L_e| \tag{63}$$

$$f^V(s_{e,l-1,nc^{e,l-1}+1})\, H^V(s_{e,l-1,nc^{e,l-1}+1}) - \sum_{j=1}^{nc_{e,l}+1} W_j^V(1)\, f^V(s_{e,l,j})\, H^V(s_{e,l,j}) = 0, \quad e \in E^E, \quad l = 2, \ldots, |L_e| \tag{64}$$

***Conditions linking upper auxiliary block to uppermost element (l = 1)* (supplementary)**

$$f_e^{VO} - \sum_{c \in C} \left(\sum_{j=1}^{nc_{e,l}+1} W_j^V(1)\, fc_c^V(s_{e,1,j}) \right) = 0, \quad e \in E^E \tag{65}$$

$$f_e^{LI} - f^L(s_{e,1,0}) = 0, \quad e \in E^E \tag{66}$$

$$f_e^{VO} x_{e,c}^{VO} - \sum_{j=1}^{nc_{e,l}+1} W_j^V(1)\, fc_c^V(s_{e,1,j}) = 0, \quad e \in E^E, \; c \in C \tag{67}$$

$$f_e^{LI} x_{e,c}^{LI} - fc_c^L(s_{e,1,0}) = 0, \quad e \in E^E, \; c \in C \tag{68}$$

$$f_e^{VO} h_e^{VO} - \sum_{j=1}^{nc_{e,l}+1} W_j^V(1)\, f^V(s_{e,1,j}) h^V(s_{e,1,j}) = 0, \quad e \in E^E \tag{69}$$

$$f_e^{LI} h_e^{LI} - f^L(s_{e,1,0}) h^L(s_{e,1,0}) = 0, \quad e \in E^E \tag{70}$$

***Conditions linking lower auxiliary block to lowermost element (l = |L_e|)* (supplementary)**

The last Finite Element of an *M/H* module is denoted by the cardinality, $|L_e|$, of set L_e.

$$f_e^{LO} - \sum_{c \in C} \left(\sum_{j=0}^{nc_{e,l}} W_j^L(M_{e,l})\, fc_c^L(s_{e,l,j}) \right) = 0, \quad e \in E^E, \; l = |L_e| \tag{71}$$

$$f_e^{VI} - f^V(s_{e,l,nc_{e,l}+1}) = 0, \quad e \in E^E, \; l = |L_e| \tag{72}$$

$$f_e^{LO} x_{e,c}^{LO} - \sum_{j=0}^{nc_{e,l}} W_j^L(M_{e,l})\, fc_c^L(s_{e,l,j}) = 0, \quad e \in E^E, \; l = |L_e|, \; c \in C \tag{73}$$

$$f_e^{VI} x_{e,c}^{VI} - fc_c^V(s_{e,l,nc_{e,l}+1}) = 0, \quad e \in E^E, \; l = |L_e|, \; c \in C \tag{74}$$

$$f_e^{LO} h_e^{LO} - \sum_{j=0}^{nc_{e,l}} W_j^L(M_{e,l})\, f^L(s_{e,l,j}) h^L(s_{e,l,j}) = 0, \quad e \in E^E, \; l = |L_e| \tag{75}$$

$$f_e^{VI} h_e^{VI} - f^V(s_{e,l,nc_{e,l}+1}) h^V(s_{e,l,nc_{e,l}+1}) = 0, \quad e \in E^E, \; l = |L_e| \tag{76}$$

***Thermodynamic functions* (supplementary)**

$$H^V(s_{e,l,j}) - H^V\left(\frac{fc^V}{f^V}, T \right)_{(s_{e,l,j})} = 0, \quad e \in E^E, \; l \in L_e, \quad j = 1, \ldots, nc_{e,l} + 1 \tag{77}$$

$$H^L(s_{e,l,j}) - H^L\left(\frac{fc^L}{f^L}, T \right)_{(s_{e,l,j})} = 0, \quad e \in E^E, \; l \in L_e, \quad j = 0, \ldots, nc_{e,l} \tag{78}$$

$$K(s_{e,l,j}) - K\left(\frac{fc_c^L}{f^L}, \frac{fc_c^V}{f^V}, T, P \right)_{(s_{e,l,j})} = 0, \quad e \in E^E, \; l \in L_e, \quad j = 1, \ldots, nc_{e,l} \tag{79}$$

GMF/Collocation Model Remarks

A main advantage of the employed collocation methods for distillation is related to the continuous problem size. Similarly to the GMF for distillation of past publications, where the size of the generated problem does not depend on the number of trays in the column but on the number of column sections (*M/H* modules), in the proposed GMF/OC and GMF/OCFE methods the problem size depends on the number of column sections and on the number of the collocation points and elements used, thus maintaining GMF's compactness. Another advantage of the proposed GMF/Collocation methods is that, for the calculation of the number of trays in each column section, no binary variables are required, thus not increasing the combinatorial size of the synthesis problems. The total number of trays per section (*M*) is a continuous variable calculated explicitly in the continuous optimization problem, thus allowing a simultaneous optimization of operating and capital cost and capturing more efficiently the interactions between the two.

From a representation perspective, the pre-specified number of collocation points per section should be sufficient for the accurate representation of the physical phenomena, but at the same time it should not be too high to lead to a substantial size increase or to numerical complexities (oscillatory behavior). However, according to the OC principles, the number of collocation points should be less than the number of trays in a column (when the design is known and operation of the column is the objective). It must be noted that in the collocation studies reported in the literature, fewer than 6 interior collocation

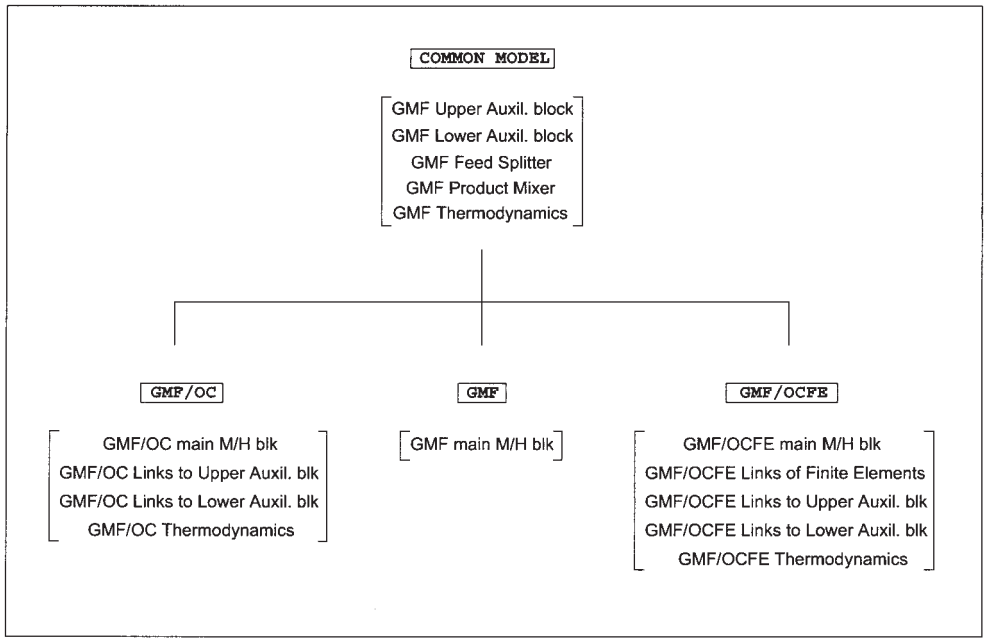

Figure 4. GMF, GMF/OC, and GMF/OCFE exchanging equation blocks.

points per section were found adequate for accurate physical representations.

From a computational point of view, the GMF and collocation methods are highly compatible due to their modular formalism, treating distillation columns section-wise. The GMF/OC and GMF/OCFE Physical Model formulations are based on *substituting* and *supplementary* constraints, replacing or being added to the existing constraints of the "*conventional*" GMF model. By using appropriate linking ("*supplementary*") equations between the Main *M/H* block and the Upper and Lower Auxiliary blocks, a "separability" feature in the model writing is created that ultimately allows the use of either the "*conventional*" GMF or each of the GMF/Collocation Physical Models by exchanging blocks of constraints, according to the level of physical representation detail required, as illustrated in Figure 4.

GMF Structural Models for Distillation Column Sequencing

The GMF Structural Model is responsible for the generation of the process alternatives during the representation/synthesis procedure. In Proios and Pistikopoulos[1] and Proios et al.,[2] appropriate GMF Structural Models were proposed for the simple, heat integrated, and complex distillation column sequencing problems, overcoming the problems' inherent structural complexities. These models are used in this work coupled to the proposed GMF/OC and GMF/OCFE Physical Models. A brief overview of the main principles of these structural models is given below. A detailed presentation and analysis of these models can be found in the aforementioned publications.

As mentioned earlier, the GMF Structural Models employ multipurpose Mass/Heat (*M/H*) and Pure Heat (*He*) modules as the *GMF Building Blocks*. Binary variables are used to denote the existence of these building blocks and of their interconnections. This formulation is employed in the GMF since it facilitates the construction of the structural models and enhances the performance of the structural optimization. The other main component of the GMF Structural Models is the *GMF Interconnection Principles*. These define the way the building blocks should be connected to each other in order to generate the structural alternatives, and they must be such that physically meaningful sequences are generated. The Interconnection Principles consist of the *GMF Structural Sets* and *GMF Structural Constraints*. The former provide information regarding available feed and desired product streams, the necessary numbers of building blocks, their topology in a superstructure, and their general allowed or forbidden interconnections. Their assignment is arranged through appropriately defined guidelines and through information derived from the problem superstructure. The GMF Structural Constraints are pure integer constraints defined over the aforementioned GMF Structural Sets and provide the problem-specific rules for the generation of distillation columns and their sequences. They can be considered as the mathematical translation of the problem superstructure, and they are incorporated in the generated MINLP problems.

For all the distillation sequencing problems examined, the GMF Structural Constraints are generated in a systematic *Three*-Stage procedure employing logical modeling. In the *1st Stage*, the GMF Structural Constraints are posed as propositional logic expressions, where the binary variables are replaced for consistency by their corresponding Boolean (logical) variables. The propositional expressions according to their function in the GMF Structural Model are categorized into Superstructure Basis, Intra-Column, and Inter-Column. The Superstructure Basis expressions provide information on the maximum or minimum number of building blocks and fix structural components that participate in all the structural alternatives. The Intra- and Inter-Column expressions are responsible for providing the necessary rules interconnecting the

Table 1. Binary Distillation Case Study[1]

System	Benzene − Toluene
Thermodynamic model	Liquid phase − ideal Vapor phase − ideal
Source of thermodynamic data	Reid[22]
Feed flowrate	$F = 100$ mol/s
Feed compositions	$x_{F,Benzene} = 0.7$ $x_{F,Toluene} = 0.3$
Column pressure	$P = 1$ atm
Feed temperature	$T_F = 359.98$ K
EMTA	10 K

GMF Building Blocks for the representation of single columns and their sequences, respectively. In the *2nd Stage*, the propositional expressions are transformed into their conjunctive normal form and into their corresponding (pure integer) GMF Structural Constraints, while replacing the Boolean variables with their corresponding binary variables. In the *3rd Stage*, the GMF Structural Sets are assigned their specific members, fully defining the GMF Structural Constraints for the particular problem examined.

It must be noted that the GMF Structural Models generated in this systematic procedure are always accurate and tight, which has proved particularly efficient for the accurate generation of all the feasible (physically meaningful) structural alternatives and the solution of the synthesis problems. This is particularly important for the GMF, which is based on building blocks of high levels of structural abstraction (where distillation columns are not represented *a priori*). Moreover, the tightness of the generated problems enhances considerably the computational efficiency of the proposed methods since the solution of each structural problem in the decomposition MINLP algorithm requires only minimum computational effort.

Validation: Distillation Column Physical Representation and Design

The proposed GMF/Collocation Physical Models were validated with respect to their accuracy and adequacy for the physical representation and design of distillation columns through a comparison to a rigorous distillation model and through the introduction of an appropriate distillation column design procedure, generating detailed and optimal design guidelines. For validation purposes the binary distillation separation of Benzene-Toluene[1] was revisited. The problem data were based on the EX5FEED test problem from Viswanathan and Grossmann[21] and are given in Table 1. The problem objective function, which was also taken from the EX5FEED test problem, considered the maximization of the difference $P1 - 50r$, where $P1$ is the flowrate of the column distillate and r is the column reflux ratio. Also, a purity specification was imposed so that $x^P_{P1,Benzene} \geq 0.99$, where $x^P_{P1,Benzene}$ is the molar fraction of benzene in the distillate.

GMF/OC distillation column model validation

The single simple distillation column was generated using two *M/H* and two *He* modules appropriately interconnected. For the GMF/OC representation, each *M/H* block was discretized using a pre-specified number of collocation points. For the type of mixture examined, 4 interior collocation points were used for the discretization of each *M/H* module. A schematic of the GMF versus the GMF/OC representation is given in Figure 5. From a Degree of Freedom analysis, it was found that using the GMF/OC Physical Model, the single simple distillation column model has 4 degrees of freedom. These correspond to 2 operation-related degrees of freedom (which are the same as those of the rigorous model of Viswanathan and Grossmann[21] for fixed design, that is, fixed number of trays) and 2 additional design-related degrees of freedom, corresponding to the number of trays per module, M_e. For simulation (fixed design) purposes, a possible pair for the 2 operational degrees of freedom could be the reflux and the purity of a component in the column distillate.

In order to validate the GMF/OC Physical Model, a *quantitative* and *qualitative* comparison was conducted over the results of both the rigorous tray-by-tray model of Viswanathan and Grossmann[21] and those of the '*conventional* ' GMF. Although, the GMF/OC can now be used for a formal optimization of the number of trays of the represented column, in order to provide a common comparison basis among the three models, the number of trays within each *M/H* block (M_1 and M_2) was fixed according to the number of trays and feed location used in the rigorous model (set to 25 trays and feed in the 11th tray from the bottom). Each one of the 4 Auxiliary Blocks (2 for each *M/H* module) was assigned to 1 tray, since these are essentially modeled as equilibrium stages. M_1 and M_2 were fixed equal to 9 and 11, respectively. The Cooler was numbered as the last tray. Therefore, *M/H* block 1 and its lower Auxiliary Block corresponded to the 10 trays below the feed. The upper Auxiliary Block of *M/H* module 1 corresponded to the feed tray (11th tray). Finally, *M/H* module 2 and the Cooler corresponded to the remaining 14 trays above the feed, as in the tray-by-tray model. However, since a comparison to the *"conventional"* GMF was also desirable, which only allows for optimization problems, the examined problem focused on the optimization of the column operation (with the objective function and specifications as given above).

The GMF/OC column model was optimized in GAMS[23] using the NLP solver CONOPT2. The *quantitative* results of the three models along with those obtained using the DSTWU

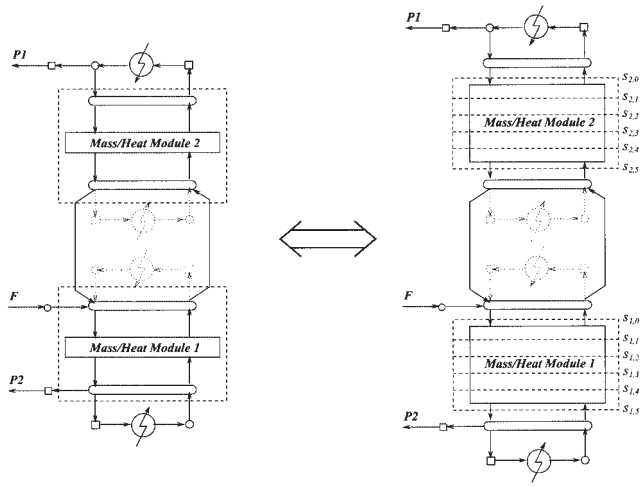

Figure 5. GMF and GMF/OC representations of a simple column.

Table 2. GMF/OC Quantitative Validation for Binary Distillation

	Qreboiler (kW)	*Qcondenser* (kW)	*P*1 (mol/s)	*r*
Shortcut	4191.7	4165.6	71.8	0.87
GMF	4194.1	4149.5	70.7	0.91
GMF/OC	4258.1	4216.8	69.6	0.96
Trayed	4401.5	4398.6	69.7	0.97

shortcut model of ASPEN PLUS, which uses the Winn-Underwood-Gilliland method, are compared in Table 2. From these results, it is apparent that the incorporation of OC principles in the GMF enhanced considerably the GMF's physical representation, providing accurate energy consumption estimates that were the closest to those of the rigorous model. The small difference in the reboiler and condenser duties between the GMF/OC and rigorous models (3% and 4%, respectively) is due to the fact that in the GMF/OC the reboiler is approximated through a Heater and the condenser through a Cooler, which are pure heat modules where no mass exchange takes place.

However, the main enhancement in the physical representation of the GMF by the incorporation of the OC principles is particularly evident when the results of the three alternative models are compared *qualitatively*. This comparison is depicted in Figure 6. From the latter it is apparent that the GMF/OC and the rigorous models are in remarkable agreement in the two sections/modules of the distillation column. The GMF enhanced with OC principles no longer captures the *general* trends of mass and heat transfer as the *"conventional"* GMF or the shortcut models, but can provide a detailed representation (intra-section information) of the physical behavior of a distillation column. This is evident in both the Benzene distribution and the column temperature profiles, where the GMF/OC and rigorous model results are virtually identical.

Another advantage of the GMF/OC model that needs to be stressed is that the above results have been obtained by a model that still remains compact in the combinatorial and continuous size. The incorporation of trays has been kept in the continuous space, avoiding the introduction of binary variables. The continuous size of the problem is larger than that of the GMF, but it is still smaller than that of the rigorous model. A size comparison of the three models is given in Table 3. It must be noted that despite the increase in the GMF problem size, the GMF/OC still maintains the GMF advantage of generating a problem whose size is independent of the number of trays, as it still depends solely on the number of column sections (*M/H* modules) and interior collocation points. For instance, if the number of trays doubles ($N = 50$), the number of equations for the rigorous model will be *557*, whereas the GMF/OC will still have the same size as the one given in Table 3.

Table 3. GMF/OC Binary Distillation Optimization Statistics

	Trayed	GMF/OC	GMF
Continuous variables	283	244	134
Continuous equalities	282	243	127

GMF/collocation distillation column design model

GMF/OC Distillation Column Design

As mentioned earlier, the incorporation of OC principles within the GMF enables the estimation of the column number of trays, leading to more detailed design guidelines. In order to achieve this goal, the optimization was extended to the GMF/OC variables that corresponded to the number of trays (M_e) for each *M/H* module. For this purpose, the optimization problem was extended to the minimization of the column's Total Annualized Cost (TAC) in order to capture the interactions between operating and capital cost. The TAC function is given below, and the capital costing correlations are taken from Douglas[4] and Luyben and Luyben[24] and can be found in the Appendix.

$$TAC = C^{op} + CCFC^{cap} \tag{80}$$

$$C^{op} = \sum_{c \in E^H} C^{st} Q_e^H y_e^H + \sum_{e \in E^C} C^{cw} Q_e^C y_e^C \tag{81}$$

$$C^{cap} = \sum_{e \in E} C_e^{col} y_e + \sum_{e \in E^H} C_e^H y_e^H + \sum_{e \in E^C} C_e^C y_e^C \tag{82}$$

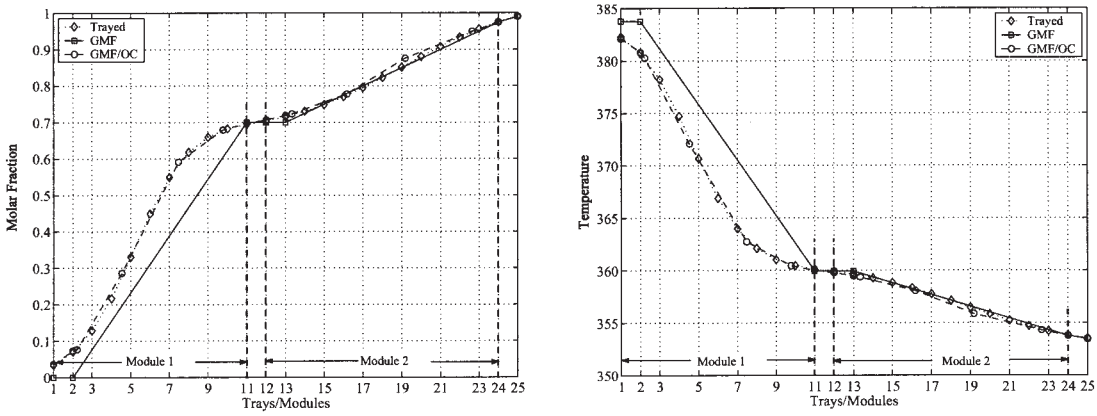

(a) Benzene Composition (b) Temperature Profile

Figure 6. GMF/OC qualitative validation for binary distillation.

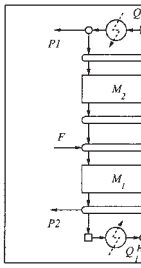

	F (mol/s)	x_{Benz}	x_{Tol}
$P1$	70.4	0.99	0.01
$P2$	29.6	0.01	0.99
	Heat Duties (kW)		
Q_1^H	4252.1		
Q_2^C	4208.5		
	Estimated Trays		
M_1	12.2		
M_2	13.4		

Figure 7. GMF/OC column optimal design and operating conditions.

Having provided an analytic relation of the Total Annualized Cost objective function to be minimized, the Benzene-Toluene case study was re-revisited for the minimization of the system's total annualized cost and with an additional specification of $x^P_{P2,Toluene} \geq 0.99$, where $x^P_{P2,Toluene}$ is the Toluene molar fraction at the bottoms. The number of degrees of freedom was increased to 4 due to the addition of the variables corresponding to the trays per each main *M/H* module (M_e).

The results from the generated NLP problem, solved in GAMS with CONOPT2 as the nonlinear solver, are given in Figure 7. The Total Annualized Cost was found equal to \$881,200/yr, from which 79% were attributed to the operating cost (\$693,900/yr) and 21% to the annualized capital cost (\$187,300/yr). A note must be made regarding the non-integer tray numbers per *M/H* module (column section). A rounding to the nearest highest integer was possible, but it was not considered necessary as the contribution to the actual TAC would have been minimal. The above results were in accord with common distillation column heuristics,[4] which estimate the contribution of annualized capital cost to around 20-30% of the TAC. Therefore, the GMF/OC design model was found able of accurately and efficiently capturing interactions between operating *and* capital cost for the design of distillation columns.

GMF/OCFE Distillation Column Design

A distillation column design model was also developed for the GMF/OCFE Physical Model. For these purposes, additional functions are incorporated corresponding to capital costing objectives for the optimization of the represented systems' Total Annualized Cost (TAC). The functions for the estimation of the latter were essentially the same as those used for the GMF/OC analysis. The only difference lay in the estimate of the capital cost of the main *M/H* modules (column sections), where Eqs. 108 and 109 were replaced by the following, allowing for the introduction of Finite Elements within each *M/H* module:

$$H_e = (2 + 0.2)\left[\sum_{l \in L_e} (M_{e,l}) + 2\right], \quad \text{(ft)} \tag{83}$$

$$H_e^{ts} = 2\left[\sum_{l \in L_e} (M_{e,l}) + 2\right], \quad \text{(ft)} \tag{84}$$

The binary distillation case study was also examined using the GMF/OCFE design model. In this problem the number of trays was also optimized along with the operating cost for the minimization of the Total Annualized Cost (TAC). For the implementation of this model, a discretization scheme for each *M/H* module of 2 Finite Elements of 2 interior Collocation Points was adopted. This discretization scheme was found sufficient for obtaining the desired accuracy in the distillation separation examined. For this discretization scheme, the number of degrees of freedom for the simple column design NLP problem increased to 6. These corresponded to the 2 operation-related simple distillation degrees of freedom (for instance, reflux ratio and distillate composition for one component) and to 4 design-related degrees (tray numbers of each of the 4 Finite Elements employed). The problem input data, objective function, and specifications were the same as those employed in the GMF/OC case. The generated problem was solved in GAMS using the CONOPT2 nonlinear solver.

The GMF/OCFE column design led to a TAC of \$872,030/yr, which was more improved from the solution obtained through the GMF/OC (\$881,200/yr). Examining closer the contribution to this TAC, it was found that the GMF/OCFE found a better solution than the GMF/OC both with respect to the operating cost (\$690,350/yr versus the \$693,900/yr of the GMF/OC) and with respect to the annualized capital cost (\$181,680/yr versus \$187,300/yr). This was due to the introduction of finite elements, which, as noted earlier, generally provides more enhanced physical representations of the examined systems. Similar to the GMF/OC results, the annualized capital cost participation in the TAC was found here equal to 20.8%, which indicated the good balance of capital and operating cost in the column design procedure through the GMF/OCFE. From a problem dimensionality point of view, the representation enhancement achieved through the incorporation of finite elements led at the same time to an increase of the problem size (8.3% in the number of equations, when compared to the GMF/OC problem), leading to the largest problem size of the GMF and GMF/Collocation models employed. Nevertheless, the generated problem's size was still smaller than that of the rigorous model and still independent of the number of trays in a column.

Examples: Synthesis of Simple, Heat Integrated, and Complex Distillation Column Sequences

The GMF/Collocation design physical models were coupled to the GMF Structural Models for the synthesis of simple, heat integrated, and complex distillation column sequences. For illustration purposes, the ternary sequencing problem of Benzene-Toluene-o-Xylene examined in Proios and Pistikopoulos[1] and Proios et al.[2] was also revisited. The problem input data, objective, and specifications are given in Tables 4 and 5. It

Table 4. Ternary Case Study Physical System Data

System	Benzene − Toluene − *o*-Xylene
Thermodynamic model	Liquid phase − ideal Vapor phase − ideal
Source of thermodynamic data	Reid[22]
Feed flowrate	$F = 1000$ kmol/hr
Feed compositions	$x_{F,Benzene} = 0.2$ $x_{F,Toluene} = 0.4$ $x_{F,o-Xylene} = 0.4$
EMTA	10 K

Table 5. Ternary Simple Column Sequencing Objectives

Objective function	min *TAC*
Benzene at product *P*1	$x^{P}_{P1,Benzene} \geq 0.95$
Toluene at product *S*	$x^{P}_{S,Toluene} \geq 0.95$
o-Xylene at product (*P*2)	$x^{P}_{P2,o-Xylene} \geq 0.5$

must be noted that higher separations (of more than 3 components) can be addressed based on the guidelines presented in the aforementioned publications. The GMF/OC model was used for the simple distillation column sequencing problem, extending the synthesis target to finding the most economical column sequence, that is, the optimal sequence with respect to both the energy consumption and the capital expenditure. For the synthesis of Heat Integrated and Complex distillation column sequences, although the GMF/OC model can be used generating accurate results, the GMF/OCFE model was instead employed, capturing in more detail the more complex physical phenomena and the operating-capital cost interactions of these systems. The synthesis results provided operation and design guidelines, not only generating the best column sequence, but also specific column dimensionality information. It is worth noting that the discretization enhancements in the GMF allowed for the *explicit* representation of complex arrangements, such as the Dividing Wall Column (DWC), exploring the potential for further cost savings. From a computational perspective, all the generated problems were Mixed Integer Nonlinear Programming (MINLP) problems implemented in GAMS and solved using the APROS/GBD methodology.[25] The Master subproblems were solved using CPLEX as the MILP solver, and the Primal subproblems were solved with CONOPT2 as the NLP solver.

GMF/OC simple column sequencing formulation and results

In this problem the GMF/OC Physical Model was coupled to the GMF Structural Model introduced in detail in Proios et al.[2] For the construction of the GMF/OC Physical Model, each *M/H* module was discretized using 6 collocation points (2 exterior and 4 interior). This discretization scheme was found adequate for the accurate representation of the underlying physical phenomena. For the mixed integer constraints $\mathcal{F}^{\max}$ was set to 1800 kmol/hr, and the problem objectives included the minimization of the sequences' TAC subject to product specifications (Table 5). According to the problem's input data, the columns' pressure was assumed constant and equal to 1 atm. The feed stream's temperature was set equal to 383.2 K, which corresponded to the bubble point at the entering module's pressure. The TAC model was the one used for the single column case, with the only difference associated to the definition of the diameter of each column, D_e. Eq. 107 was replaced by equations defining uniform diameters for *M/H* modules belonging to the same column:

$$D_e = 0.1838(f^{HV}_{1,1})^{0.5}, \quad e = 1, 2 \tag{85}$$

$$D_e = 0.1838(f^{HV}_{3,3})^{0.5}, \quad e = 3, 4 \tag{86}$$

$$D_e = 0.1838(f^{HV}_{5,5})^{0.5}, \quad e = 5, 6 \tag{87}$$

From the solution of the synthesis problem, the optimal solution was found, as in Proios et al.[2] in 2 GBD iterations and corresponded to the Direct Sequence. In the GBD algorithm, the Direct Sequence was the initial structure to be evaluated. The *1*st Master generated the Indirect Sequence and the *2*nd Master the 3-Column Sequence, which was not evaluated since the algorithm convergence criterion was met (upper-lower bound crossing). The optimal design and operating conditions for the examined sequencing problem are given in Figure 8. The TAC of the sequence was found equal to \$2,912,500/yr, which consisted of an Operating Cost of \$2,431,900/yr (83% contribution to the TAC) and of an Annualized Capital Cost of \$480,600/yr (17% contribution to the TAC).

From a comparison of the results obtained with the GMF/OC to those of the GMF, it is apparent that the former enhanced model can now provide detailed design guidelines, which include not only energy consumption information but are extended to the actual sequence design (number of trays, diameter). Comparing the solutions obtained between the GMF and GMF/OC models, it is noted that the former, indeed, provided a lower bound on the operating cost (equal to \$2,369,000/yr versus the \$2,431,900/yr of the GMF/OC). This difference of 2.6%, which is due to the trading off between operating and capital cost in the GMF/OC model, also demonstrated the validity of the original GMF Physical Model, which captured the physical behavior and the energy efficiency of the represented sequences using an aggregated model.

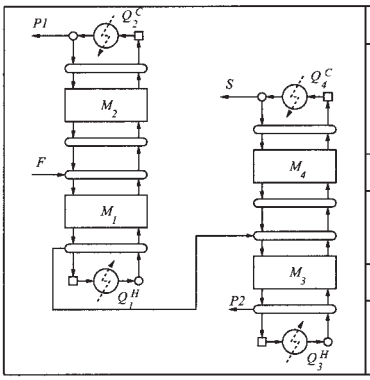

	F $(kmol/hr)$	x_{Benz}	x_{Tol}	x_{o-Xyl}
$P1$	210.5	0.95	0.05	0
S	388.9	0	0.95	0.05
$P2$	400.6	0	0.05	0.95
	Column 1		***Column 2***	
Trays	M_1=25.8 M_2=5.6		M_3=11.3 M_4=8.2	
D_e (ft)	7.12		7.67	
Q_e^H (kW)	6860.3		8090.4	
Q_e^C (kW)	6562.2		7934.4	

Figure 8. GMF/OC simple column sequencing optimal design and operation.

Table 6. GMF/OCFE *HI* Column Sequencing GBD Convergence History

Iter.	Primal	Master
1	2.868 10^6	0.349 10^6
2	2.801 10^6	1.102 10^6
3	2.398 10^6	1.638 10^6
4	2.126 10^6	1.892 10^6
5	1.974 10^6	2.040 10^6

GMF/OCFE HI *column sequencing formulation and results*

As noted earlier, the GMF/OCFE Physical Model was coupled to the GMF Structural Model for the Heat Integrated (*HI*) simple column sequencing problem. The GMF Structural Model for the ternary sequencing problem examined was also taken from Proios et al.,[2] where the problem superstructure, propositional logic expressions, and their corresponding pure integer constraints were given in detail. For the GMF/OCFE Physical Model, each *M/H* module was discretized into 2 Finite Elements of 2 interior collocation points each. Furthermore, column pressure, which is one of the most important operating parameters for heat integration, was *explicitly* incorporated as an optimization variable, as opposed to the shortcut models that consider column pressure only implicitly. This enhanced the physical representation of the *HI* schemes, allowing for the direct capture of the effects of pressure on distillation heat integration. Since in the *HI* case the column pressure is considered an additional degree of freedom, the pressure that participated in the OCFE constraints was set equal to that of each *M/H* module. A pressure drop profile was not employed for simplicity reasons, however, without affecting the validity of the results. In the mixed integer physical-structural constraints, $\mathcal{F}^{\max}$ was set to 1800 kmol/hr. The synthesis objectives included the minimization of TAC, subject to the product purity specifications of Table 5. For the *HI* case, the TAC model of the GMF/OCFE simple column sequencing method incorporated the capital cost of the *HI* blocks, as shown below. The capital costing correlations can be found in the Appendix.

$$C^{cap} = \sum_{e\in E} C_e^{col} y_e + \sum_{e\in E^H} C_e^H y_e^H + \sum_{e\in E^C} C_e^C y_e^C + \sum_{e,ea\in E^X} C_{e,ea}^{HI} y_{e,ea}^{HI} \tag{88}$$

From the solution of this more involved synthesis problem, the optimal design was obtained in 5 GBD iterations and corresponded to a Heat Integrated variant of the Direct Sequence. The optimal configuration, along with its design and operating parameters, is shown in Figure 9. The TAC at the optimal solution was found equal to \$1,974,400/yr, consisting of an Operating Cost of \$1,420,900/yr (72% of the TAC) and an Annualized Capital Cost of \$553,500/yr (28% of the TAC). From a comparison to the *non-HI* optimal sequence and design, the Heat Integration provided annual savings of 32% (corresponding to \$938,100/yr). From a closer investigation it was found that this improvement was due to a substantial decrease of the Operating Cost, which has been reduced to 42% due to the *HI* of the two columns. This has been achieved by increasing the pressure in the first column of the sequence so that its condenser could be Heat Integrated with the reboiler of the second column. The GMF/OCFE captured these effects directly and accurately by incorporating pressure *explicitly* in the optimization problem solved.

From a comparison with the optimal solution provided by the *"conventional"* GMF[2] for the same problem, it was found that both synthesis frameworks have resulted in the same optimal sequence, with the same Heat Integration scheme. The GMF, as expected, provided a lower bound of the Operating Cost, namely \$1,392,000/yr[2] versus \$1,420,900/yr of the GMF/OCFE. The reason that both frameworks have resulted in the same structure and in comparable operating costs (even when GMF/OCFE takes into account capex interactions) is that the main driving force in the examined optimization problem is the operating cost, which makes *by far* the dominant contribution into the examined distillation system's expenditure.

From a computational point of view, the optimal structure was found in 5 GBD iterations. The convergence history is given in Table 6. Starting from the *non-HI* optimal sequence (Direct Sequence), the 2nd and 3rd GBD iterations corresponded to *HI* variants of the Indirect Sequence. The final two iterations (4th and 5th) corresponded to *HI* variants of the Direct Sequence. Convergence was achieved in the 5th iteration when the lower bound of the 5th Master subproblem crossed the current best upper bound.

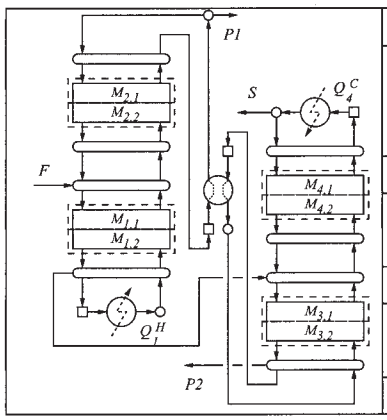

	F $(kmol/hr)$	x_{Benz}	x_{Tol}	x_{o-Xyl}
$P1$	190.05	0.95	0.05	0
S	388.9	0.05	0.95	0
$P2$	421.05	0	0.05	0.95
	Column 1		***Column 2***	
Trays	$M_{1,1}$=5.2, $M_{1,2}$=11.4		$M_{3,1}$=2.2, $M_{3,2}$=2.4	
	$M_{2,1}$=3.7, $M_{2,2}$=5		$M_{4,1}$=2.1, $M_{4,2}$=10.3	
D_e (ft)	7.81		7.61	
Q_e^H (kW)	8276.3		-	
Q_e^C (kW)	-		10873.8	
P_e (atm)	6.13		1	

Figure 9. GMF/OCFE *HI* simple column sequencing optimal design and operation.

GMF/OCFE complex column sequencing formulation and results

For the complex distillation column sequencing problem, the GMF/OCFE Physical Model was coupled to the GMF Structural Model, which was introduced along with the presentation of the structural alternatives in Proios and Pistikopoulos[1] for the separation of a ternary mixture into its constituent components. As posed in the literature, the problem's structural alternatives include both simple and complex column sequences. For the ternary sequencing problem, the same input data, objective, and specifications were used as in the sequencing problems examined already. Since no heat integration techniques are incorporated, as in the simple distillation sequencing case, the columns' pressure was set to 1 atm and the feed stream temperature to 383.2 K. The GMF/OCFE Physical Model was formulated using the 2 Finite Element-2 Interior Collocation point discretization scheme for each *M/H* module. For the mixed integer constraints $\mathcal{F}^{\max}$ was set equal to 1800 kmol/hr. The Total Annualized Cost model was the same as the one defined in the simple column sequencing problem. For the complex distillation column sequencing case, the only particularities were found in the *M/H* module diameter (D_e) and height (H_e) of the *complex* column alternatives, whose definition was more involved. For the complex columns, the new diameter and height definitions are given below for each *M/H* module. *Note*: In the specifications below if the diameter or height are not re-defined, then Eqs. 85 to 87 and 108, respectively, for the diameter and height should hold; in the simple column alternatives, these hold by default. The sequences' GMF Building Block numbering can be found in the problem superstructure in detail in Proios and Pistikopoulos.[1]

Prefractionator and SL Column

$$D_e = 0.1838(f_{3,3}^{HV})^{0.5}, \quad e = 3, 4, 5, 6 \tag{89}$$

$$H_e = 2\left(\sum_{l\in L_e} M_{e,l} + 2\right), \quad e = 4, 5 \tag{90}$$

Petlyuk and RV Column

$$D_e = 0.1838(f_{3,1}^{VV})^{0.5}, \quad e = 1,2 \tag{91}$$

$$D_e = 0.1838(f_{3,3}^{HV})^{0.5}, \quad e = 3, 4, 5, 6 \tag{92}$$

$$H_e = 2\left(\sum_{l\in L_e} M_{e,l} + 2\right), \quad e = 4, 5 \tag{93}$$

Side Stripper

$$D_e = 0.1838(f_{1,1}^{HV})^{0.5}, \quad e = 1, 2, 6 \tag{94}$$

$$D_e = 0.1838(f_{5,5}^{HV})^{0.5}, \quad e = 5 \tag{95}$$

$$H_e = 2\left(\sum_{l\in L_e} M_{e,l} + 2\right), \quad e = 2 \tag{96}$$

$$H_e = (2 + 0.4)\left(\sum_{l\in L_e} M_{e,l} + 2\right), \quad e = 5 \tag{97}$$

Side Rectifier

$$D_e = 0.1838(f_{3,3}^{HV})^{0.5}, \quad e = 1, 2, 3 \tag{98}$$

$$D_e = 0.1838(f_{3,4}^{VV})^{0.5}, \quad e = 4 \tag{99}$$

$$H_e = 2\left(\sum_{l\in L_e} M_{e,l} + 2\right), \quad e = 1 \tag{100}$$

$$H_e = (2 + 0.4)\left(\sum_{l\in L_e} M_{e,l} + 2\right), \quad e = 4 \tag{101}$$

In the Prefractionator, Petlyuk, RV, and SL Columns, for the main column (*M/H* modules *3-6*) the diameter is related to the column boil-up ($f_{3,3}^{HV}$), and the height of *M/H* modules *3* and *4* is equal to that of the internals, since these are intermediate sections in the aforementioned columns. In the Petlyuk and RV columns, the diameter of the prefractionation column (*M/H* modules *1-2*) is related to the vapor interconnection ($f_{3,1}^{VV}$). For the Side Stripper *M/H* modules *1*, *2*, and *6* belong to the same column whose diameter is related to the column boil-up ($f_{1,1}^{HV}$) and *M/H* module *2* is an intermediate section. However, *M/H* module *5* is a side column with additional height due to existing top and bottom sections and with its diameter defined by Eq. 87. Similar considerations are made for the Side Rectifier Sequence, where the *M/H* modules *1*, *2*, and *3* belong to the same column, with *M/H* module *2* an intermediate section and *M/H* module *4* a separate side column. In the GAMS implementation, the aforementioned correlations were incorporated using Dollar Operators, \$.

The solution of the MINLP problem corresponded to the Petlyuk Sequence. The Total Annualized Cost of the Petlyuk Column was found equal to \$2,075,100/yr, which corresponded to operating cost of \$1,657,200/yr and annualized capital cost of \$417,900/yr. The optimal design with the optimized operating conditions is given in Figure 10.

From a computational point of view, convergence was achieved in 4 GBD iterations, from which the optimal solution corresponded to the solution of the 2nd Primal subproblem, as can be seen in Table 7. The initial structure to be evaluated (1st Primal) was the best simple column solution (Direct Sequence). The second sequence generated and evaluated corresponded to the Petlyuk column, whereas the 3rd and 4th iterations generated the suboptimal Side Stripper and Side Rectifier Sequences. It must, however, be noted that the GMF in Proios and Pistikopoulos[1] found the Petlyuk column as the optimal sequence, in the same number of iterations and in the same sequence generation per GBD iteration.

From the results obtained, some very interesting conclusions can be made regarding the ternary distillation problem examined. Namely, if the Petlyuk sequence is compared to the optimal simple column sequence (the direct sequence), it can be found that the former provides savings of \$837,400/yr, corresponding to an improvement of 29% in the separation economics. This is due to large savings both in the operating

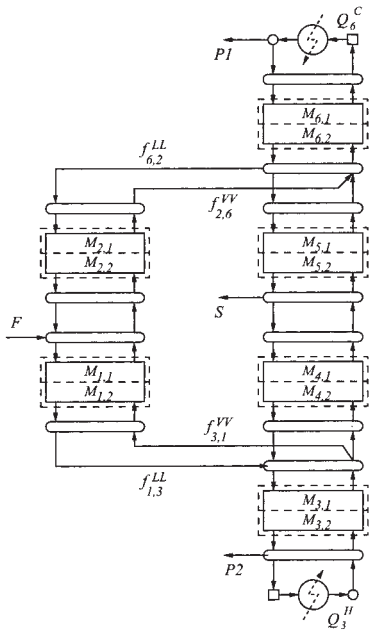

	$F(kmol/hr)$	x_{benz}	x_{tol}	x_{o-xyl}
$P1$	207.5	0.95	0.05	0
S	388.9	0.007	0.95	0.043
$P2$	403.6	0	0.05	0.95
$f_{6,2}^{LL}$	220.4	0.25	0.731	0.019
$f_{2,6}^{VV}$	592.4	0.425	0.552	0.023
$f_{3,1}^{VV}$	585.3	0.009	0.755	0.237
$f_{1,3}^{LL}$	1213.3	0.007	0.557	0.436

	Prefrac.	***Main***
Trays		$M_{6,1}$=2.1, $M_{6,2}$=2.1
	$M_{2,1}$=4.7, $M_{2,2}$=2.5	$M_{5,1}$=2.9, $M_{5,2}$=2.6
	$M_{1,1}$=5.1, $M_{1,2}$=2.3	$M_{4,1}$=5.7, $M_{4,2}$=2.3
		$M_{3,1}$=4.6, $M_{3,2}$=3.8
D_e	6.602	8.612
Q_e^H	-	10211.2
Q_e^C	-	9757.8

Figure 10. GMF/OCFE complex column sequencing optimal design and operation.

cost (32%) and in the capital cost (13%). However, by comparing the Petlyuk column to the best Heat Integrated simple column sequence (*HI* Direct Sequence), it is found that, for the examined problem, Heat Integration leads to a better economic performance than that of Full Thermal Coupling. The total annual expenditure of the *HI* sequence is \$100,700/yr less than that of the Petlyuk column, corresponding to a TAC difference of 5%. From the corresponding results, the *HI* sequence produced more operating cost savings, whereas the complex column more capital expenditure savings. The close performance of these alternatives can demonstrate the importance of using synthesis tools that can generate all these alternatives in a unified way and can then evaluate them in order to provide the most cost efficient design.

GMF/OCFE dividing wall considerations

The Dividing Wall Column (DWC) is essentially a side stream column that has a vertical wall splitting its middle section in two separate compartments. Under the assumption of no heat transfer through the vertical wall, the DWC is considered thermally equivalent to the Petlyuk column, therefore encompassing the same thermal coupling effects and generating equivalent energy savings. However, it also provides capital cost savings by including the main and the prefractionation columns of the Petlyuk arrangement in the same shell. In Proios and Pistikopoulos,[1] since the GMF did not incorporate intra-module information, the DWC was *implicitly* considered for its energy efficiency, using its thermally equivalent Petlyuk column. In this work, the representational enhancement of the GMF with orthogonal collocation principles allowed the *explicit* representation and evaluation of the DWC with respect to its Total Annualized Cost. This was achieved in a 2-step optimization procedure. The first step is the solution of the complex column sequencing problem, as described earlier. If this has the Petlyuk Column as its optimal solution, then a second step is introduced that involves the optimization of the DWC. If the solution of the first step is not the Petlyuk Column, then the DWC is not evaluated. This utilizes the fact that in the examined distillation separation, the operating cost is the main economic driving force and, if the Petlyuk column is suboptimal with respect to the latter, then the capital cost savings of its thermally equivalent DWC cannot compensate for the suboptimal energy savings. An alternative way of including the DWC in the structural model is by incorporating an additional binary variable designating if the prefractionating column is fitted within the main column shell, as specified in Dunnebier and Pantelides.[26]

Table 7. GMF/OCFE Complex Column Sequencing GBD Convergence History

Iter.	Primal	Master
1	2.868 10^6	0.205 10^6
2	2.075 10^6	1.102 10^6
3	2.434 10^6	1.769 10^6
4	2.637 10^6	2.423 10^6

In order to model the DWC starting from the Petlyuk design, the following conditions are imposed: (*i*) The number of trays in the prefractionation column (*M/H* modules *1* and *2*) must be equal to those in the intermediate sections of the main column (*M/H* modules *4* and *5*); (*ii*) the diameter of these *4 M/H* modules should be approximately half of that in *M/H* modules *3* and *6* so that the column has a uniform diameter; and (*iii*) the height (H_e) of *M/H* modules *1*, *2*, *4*, and *5* is calculated using the intermediate section definition (Eq. 93), whereas for the remaining *M/H* modules Eq. 108 holds. These conditions are given below:

$$\sum_{l\in L_1} M_{1,l} + \sum_{l\in L_2} M_{2,l} - \sum_{l\in L_4} M_{4,l} - \sum_{l\in L_5} M_{5,l} = 0 \qquad (102)$$

$$D_1 = D_2 = D_4 = D_5 = D_3/2 \qquad (103)$$

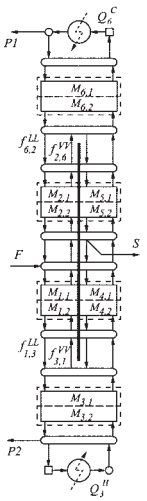

	$F(kmol/hr)$	x_{benz}	x_{tol}	x_{o-xyl}
$P1$	208.9	0.95	0.05	0
S	388.9	0.004	0.95	0.046
$P2$	402.2	0	0.05	0.95
$f^{LL}_{6,2}$	245.3	0.253	0.726	0.021
$f^{VV}_{2,6}$	643.8	0.405	0.572	0.023
$f^{VV}_{3,1}$	635.1	0.004	0.757	0.239
$f^{LL}_{1,3}$	1236.6	0.003	0.559	0.438

Column Design	
Trays	$M_{6,1}$=2.1, $M_{6,2}$=2.1
	$M_{2,1}$=5.4, $M_{2,2}$=3.4, $M_{5,1}$=4.3, $M_{5,2}$=3.4
	$M_{1,1}$=4.3, $M_{1,2}$=3.3, $M_{4,1}$=5.4, $M_{4,2}$=3.3
	$M_{3,1}$=4.6, $M_{3,2}$=3.8
D_e	$D_{3,6}$=8.6, $D_{1,2,4,5}$=4.3
Q^H_e	10126.5
Q^C_e	9672.8

Figure 11. GMF/OCFE dividing wall column optimal design and operation.

$$H_e = 2\left[\sum_{l\in L_e} M_e + 2\right], \quad e = 1, 2, 4, 5 \tag{104}$$

$$H_e = (2 + 0.2)\left[\sum_{l\in L_e} M_e + 2\right], \quad e = 3, 6 \tag{105}$$

Having incorporated the above structural particularities in the GMF/OCFE Physical Model of the DWC, the generated design NLP problem was solved in GAMS for the minimization of the system's TAC. The GMF DWC structural representation along with the GMF/OCFE optimization with respect to the column design and operating conditions results is given in Figure 11. The TAC of the DWC was found equal to \$1,983,600/yr, which corresponded to an operating cost of \$1,643,400/yr and to an annualized capital cost of \$340,200/yr. Therefore, the DWC was found as the most economical complex column, with annual savings of \$91,500/yr in comparison to the Petlyuk column. The main contribution to this improvement was related to the capital expenditure of the DWC, which is related to its capital cost savings by achieving this separation from one column, while the operating cost (energy consumption) of the two columns was found equivalent, which validated the thermal equivalence assumption. However, from a comparison to the best Heat Integrated simple column, the latter still remained the most economical design, though by a small margin (\$9100/yr).

Conclusions

In previous work, GMF Synthesis Models have been developed for the synthesis of distillation column sequences involving simple, heat integrated, and complex columns. The task in this article was the enhancement of the above models by incorporating in the GMF Physical Model principles from the Orthogonal Collocation (OC) and Orthogonal Collocation on Finite Elements (OCFE) methods for order reduction. Two synthesis frameworks were appropriately introduced, namely, the GMF/OC and the GMF/OCFE, allowing for detailed representations of the underlying physical phenomena and sequencing design information, maintaining the GMF's main advantages of continuous and combinatorial compactness while avoiding the use of common simplifying assumptions. The proposed GMF/Collocation Synthesis Models, based on the modular formalism of both the GMF and collocation methods, were appropriately implemented, allowing the selection of the model to utilize according to the synthesis targets and the representation detail desired (GMF for conceptual design studies for energy efficiency and GMF/Collocation models for detailed design studies for overall cost efficiency).

The GMF/Collocation physical representations were validated to a binary distillation separation through a comparison to a shortcut and to a rigorous tray-by-tray model. The obtained results were virtually identical to those of the rigorous model, demonstrating the significant representational enhancement achieved while still generating compact optimization problems. A detailed design procedure was employed, capturing simultaneously the interactions between operating and capital cost in the *continuous* optimization stage. This procedure was also incorporated for the synthesis of simple, heat integrated, and complex distillation column sequences, where the GMF/Collocation Physical Models were coupled to appropriate GMF Structural Models. The solution of the generated MINLP problems provided the most cost efficient distillation column sequences, along with detailed column design and operation guidelines. The obtained results demonstrated the overwhelming economic benefits by employing Heat Integration and Thermal Coupling techniques in distillation sequence design instead of the traditional simple column designs. Moreover, the incorporation of collocation techniques in the GMF allowed the *explicit* representation of particular designs, such as the Dividing Wall Column, and captured accurately their economic benefits.

The above enhancements were achieved while keeping the problem size small and independent of the number of trays in each column and without the introduction of additional binary variables denoting the existence of trays. The GMF/OCFE, despite adding a slight representational complexity and increase of the problem size, obtained improved designs from an economic point of view, which is related to the accuracy increase through the incorporation of Finite Elements. Overall, the coupling of collocation techniques to the GMF can be viewed as the incorporation of elements of a simulation tool within the GMF conceptual design tool, while keeping intact the latter's representational advantages and compactness. For these reasons, the proposed synthesis methods can be viewed as an accurate and efficient balance between rigorous and shortcut methods for the synthesis of the examined nonazeotropic distillation column systems. Ongoing research is focused on an extension of the proposed framework utilizing principles of past work[27] for the synthesis of non-ideal reactive-separating systems.

Acknowledgments

The authors gratefully acknowledge the financial support of the OPT-ABSO European Project (G1RD-CT-2001–00649).

Notation

y = binary variable
f = molar flowrate

x = molar fraction
T = temperature
P = pressure
h = enthalpy
Q = heat load
K = phase equilibrium constant
$\mathcal{F}^{max}$ = molar flowrate upper bound
E = set of available *M/H* modules
E^E = set of existing *M/H* module at each Primal subproblem
E^H = set of available Heater modules
E^C = set of available Cooler modules
E^{HI} = set of available Heat Integration (*HI*) blocks

Subscripts

e, ea = module
i = feedstream
c = component
p = product stream

Superscripts

H = heater
C = cooler
CI = cooler module vapor inlet stream
CO = cooler module liquid outlet stream
HI = heater module liquid inlet stream
HO = heater module vapor outlet stream
LI = main *M/H* module liquid inlet stream
LO = main *M/H* module liquid outlet stream
VI = main *M/H* module vapor inlet stream
VO = main *M/H* module vapor outlet stream
VA = upper auxiliary block vapor outlet stream
LA = lower auxiliary block liquid outlet stream
FL = feed liquid interconnection
CP = cooler liquid product stream
LP = lower auxiliary block liquid product stream
LH = lower auxiliary block-heater liquid interconnection
VV = upper auxiliary block vapor interconnection (between *M/H* modules)
LL = lower auxiliary block liquid interconnection (between *M/H* modules)
VC = upper auxiliary block-cooler vapor interconnection
CL = cooler-upper auxiliary block liquid interconnection

Literature Cited

1. Proios P, Pistikopoulos EN. Generalized modular framework for the representation and synthesis of complex distillation column sequences. *Ind and Eng Chemistry Res.* 2005;44:4656-4675.
2. Proios P, Goula NF, Pistikopoulos EN. Generalized modular framework for the synthesis of heat integrated distillation column sequences. *Chem Eng Sci.* 2005;60:4678-4701.
3. Papalexandri KP, Pistikopoulos EN. Generalized modular representation framework for process synthesis. *AIChE Journal.* 1996;42:1010-1032.
4. Douglas JM. *Conceptual Design of Chemical Processes*. New York: McGraw-Hill; 1988.
5. Smith EM. On the optimal design of continuous processes. Ph.D. Dissertation, Imperial College London, London, UK, 1996.
6. Cho YS, Joseph B. Reduced-order steady-state and dynamic models for separation processes. *AIChE J.* 1983;29:261-269.
7. Cho YS, Joseph B. Reduced-order steady-state and dynamic models for separation processes—Part II. Application to nonlinear multicomponent systems. *AIChE J.* 1983;29:270-276.
8. Cho YS, Joseph B. Reduced-order steady-state and dynamic models for separation processes—Part III. Application to columns with multiple feeds and sidestreams. *Computers & Chem Eng.* 1984;8:81-90.
9. Stewart WE, Levien KL, Morari M. Simulation of fractionation by orthogonal collocation. *Chem Eng Sci.* 1985;40:409-421.
10. Wahl EF, Marriott P. Understanding and predictions of the dynamic behaviour of distillation columns. *Ind Eng Chemistry Process Design and Development.* 1970;9:396-407.
11. Georgakis C, Stoever MA. Time domain order reduction of tridiagonal dynamics of staged processes—I. Uniform lumping. *Chem Eng Sci.* 1982;37:687-697.
12. Benallou A, Seborg DE, Mellichamp DA. Low order, physically lumped dynamic models for distillation column control: Paper 9e, AIChE Annual Meeting, Los Angeles, CA; 1982.
13. Swartz CLE, Stewart WE. A collocation approach to distillation column design. *AIChE J.* 1986;32:1832-1838.
14. Swartz CLE, Stewart WE. Finite-element steady state simulation of multiphase distillation. *AIChE J.* 1987;33:1977-1985.
15. Seferlis P, Hrymak AN. Optimization of distillation units using collocation models. *AIChE J.* 1994;40:813-825.
16. Seferlis P, Hrymak AN. Adaptive collocation on finite elements models for the optimization of multistage distillation units. *Chem Eng Sci.* 1994;49:1369-1382.
17. Huss RS, Westerberg AW. Collocation methods for distillation design. 1. Model description and testing. *Ind Eng Chemistry Res.* 1996;35:1603-1610.
18. Huss RS, Westerberg AW. Collocation methods for distillation design. 2. Applications for distillation. *Ind Eng Chemistry Res.* 1996;35:1611-1623.
19. Zhang L, Linninger AA. Temperature collocation algorithm for fast and robust distillation design. *Ind Eng Chemistry Res.* 2004;43:3163-3182.
20. Van Dongen DB, Doherty MF. Design and synthesis of homogeneous azeotropic distillations. 1. Problem formulation for a single column. *Ind Eng Chemistry Res.* 1985;24:454-463.
21. Viswanathan J, Grossmann IE. Optimal feed locations and number of trays for distillation columns with multiple feeds. *Ind Eng Chemistry Res.* 1993;32:2942-2949.
22. Reid RC. *The Properties of Gases and Liquids*. New York: McGraw-Hill; 1987.
23. Brooke A, Kendrick D, Meeraus A, Raman R. *GAMS—A User's Guide*. South San Francisco, CA: Scientific Press; 2003.
24. Luyben ML, Luyben WL. Design and control of a complex process involving two reaction steps, three distillation columns and two recycle streams. *Ind Eng Chemistry Res.* 1995;34:3885-3898.
25. Paules GE, Floudas CA. APROS: Algorithmic development methodology for discrete-continuous optimization problems. *Operations Res.* 1989;37:902-915.
26. Dünnebier G, Pantelides CC. Optimal design of thermally coupled distillation columns. *Ind Eng Chemistry Fundamentals.* 1999;38:162-176.
27. Ismail SR, Proios P, Pistikopoulos EN. Modular synthesis framework for combined separation/reactive systems. *AIChE J.* 2001;47:629-650.
28. Paterson WR. A replacement for the logarithmic mean. *Chem Eng Sci.* 1984;39:1635-1636.

Appendix: Capital Costing Model

For the minimization of the column's Total Annualized Cost (TAC), the capital costing correlations of Douglas[4] and Luyben and Luyben[24] were incorporated within the GMF/Collocation framework. The Capital Charge Factor (CCF) in this work was taken equal to (1/3). The model for the Capital Costing of each *M/H* module (column section) (C_e^{col}) is given below. (*Note*: For validation purposes the units are kept as in the original publications.)

$$C_e^{col} = \frac{M\&S}{280}\left[101.9D_e^{1.066}H_e^{0.802}(2.18 + Fc) + 4.7D_e^{1.55}H_e^{ts}Fc\right] \tag{106}$$

$$D_e = 0.1838(f_{ea,ea}^{HV})^{0.5}, \quad \text{(ft)} \tag{107}$$

$$H_e = (2 + 0.2)(M_e + 2), \quad \text{(ft)} \tag{108}$$

$$H_e^{ts} = 2(M_e + 2), \quad \text{(ft)} \tag{109}$$

In the above expressions, the Marshall and Swift index (M&S) was taken equal to 1108.1 and the Correction Factor (Fc) equal to 1. Eq. 107, which was taken from Luyben and Luyben,[24] uses a correlation calculating the *M/H* module diameter with respect to the column boil-up (*Note*: the boil-up must be given in lbmol/hr, for which the correlation is defined). The boil-up in GMF terms is the vapor interconnection, $f^{HV}_{ea,ea}$, between the (column) Heater and its associated Lower *M/H* module. For simplicity reasons, the diameter was assumed uniform throughout the column and was equal to that of the lower *M/H* module (representing the stripper section). Equation 108 gives the height of each *M/H* module, and it is based on 2 ft spacing per tray and 20% more for base level.[24] In the GMF/OC formalism, $M_e + 2$ is the overall number of trays per *M/H* module (M_e trays in the main *M/H* block and 2 trays corresponding to the two Auxiliary blocks, which are essentially modeled as trays). H^{ts}_e is the height of the tray stacks in each *M/H* module (equal to tray spacing multiplied by the number of trays). Furthermore, the capital costing model for the heat units is specified below:

$$C^H_e = \frac{M\&S}{280}\,101.3(2.29 + Fc)(A^H_e)^{0.65} \tag{110}$$

$$A^H_e = \frac{Q^H_e}{11250}, \quad (\text{ft}^2) \tag{111}$$

$$C^C_e = \frac{M\&S}{280}\,101.3(2.29 + Fc)(A^C_e)^{0.65} \tag{112}$$

$$A^C_e = \frac{Q^C_e}{150\ LMTD^C_e}, \quad (\text{ft}^2) \tag{113}$$

$$LMTD^C_e = \frac{2}{3}(\Delta T1^C_e)^{0.5}(\Delta T2^C_e)^{0.5} + \left(\frac{\Delta T1^C_e + \Delta T2^C_e}{6}\right) \tag{114}$$

$$\Delta T1^C_e = T^{CI}_e - Tw \tag{115}$$

$$\Delta T2^C_e = T^{CO}_e - Tw \tag{116}$$

According to Douglas,[4] for the Heater module area the following simplification was used: $U^H\ LMTD^H \sim 11250$ Btu/hr ft^2. An analytic relation of the logarithmic mean average temperature was not employed, since after its implementation it was found that it did not make significant difference in the results, while adding complexity in the calculations. *Note*: In Eqs. 111 and 112, the heat duties must be given in Btu/hr for use in the above relations. In Eq. 112, the overall heat transfer coefficient was taken equal to 150 Btu/hr ft^2F,[24] and the Cooler module's logarithmic mean average temperature ($LMTD^C_e$) was analytically calculated using the Paterson approximation.[28] (*Note*: In Eqs. 115 and 116, the temperature units must be given in *F*.)

For the synthesis of Heat Integrated distillation column sequences, appropriate arrangements and additional capital costing correlations were introduced to the above model in order to incorporate the existence of the *HI* blocks. These are given below:

$$D_e = 0.1838\left(f^{HV}_{1,1} + \sum_{ea \in E^{XCE}_1} f^{XV}_{1,ea}\right)^{0.5,} \quad e = 1, 2 \tag{117}$$

$$D_e = 0.1838\left(f^{HV}_{3,3} + \sum_{ea \in E^{XCE}_3} f^{XV}_{3,ea}\right)^{0.5}, \quad e = 3, 4 \tag{118}$$

$$D_e = 0.1838\left(f^{HV}_{5,5} + \sum_{ea \in E^{XCE}_5} f^{XV}_{5,ea}\right)^{0.5}, \quad e = 5, 6 \tag{119}$$

$$C^{HI}_{e,ea} = \frac{M\&S}{280}\,101.3(2.29 + Fc)(A^{HI}_{e,ea})^{0.65} \tag{120}$$

$$A^{HI}_{e,ea} = \frac{Q^{HI}_{e,ea}}{150\ LMTD^{HI}_{e,ea}}, \quad (\text{ft}^2) \tag{121}$$

$$LMTD^{HI}_{e,ea} = \frac{2}{3}(\Delta T1^{HI}_{e,ea})^{0.5}(\Delta T2^{HI}_{e,ea})^{0.5} + \left(\frac{\Delta T1^{HI}_{e,ea} + \Delta T2^{HI}_{e,ea}}{6}\right) \tag{122}$$

$$\Delta T1^{HI}_{e,ea} = T^{XHI}_{e,ea} - T^{XCO}_{e,ea} \tag{123}$$

$$\Delta T2^{HI}_{e,ea} = T^{XHO}_{e,ea} - T^{XCI}_{e,ea} \tag{124}$$

The capital costing of the *HI* blocks was calculated analytically through the Logarithmic Mean Temperature Difference calculation, and Eqs. 117 to 119 provided the diameter-boil-up correlations, adjusted for the incorporation of potential contributions to the columns' boil-up from Heaters and/or *HI* blocks.

Manuscript received May 5, 2005, and revision received Sept. 6, 2005.